

Controllable Uniform Green Light Emitters Enabled by Circular HEMT-LED Devices

Volume 10, Number 05, September 2018

Yuefei Cai, *Member, IEEE*

Yipin Gong

Jie Bai

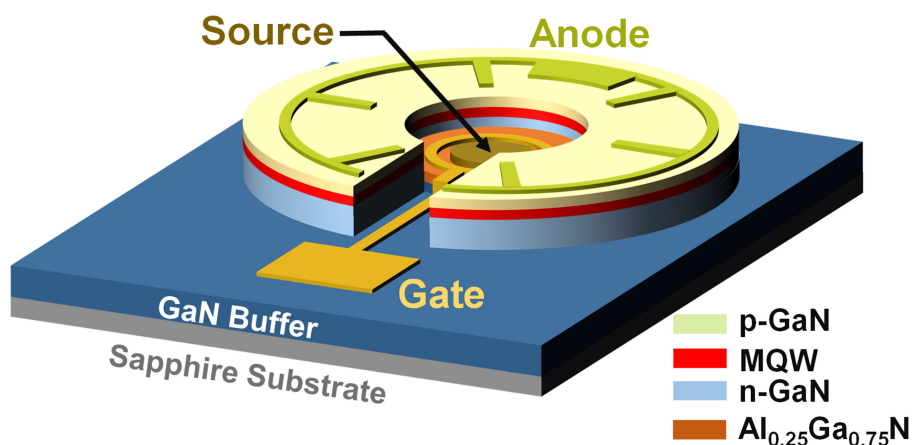
Xiang Yu

Chenqi Zhu

Volkan Esendag

Kean Boon Lee

Tao Wang



DOI: 10.1109/JPHOT.2018.2867821

1943-0655 © 2018 CC BY

Controllable Uniform Green Light Emitters Enabled by Circular HEMT-LED Devices

Yuefei Cai , Member, IEEE, Yipin Gong, Jie Bai , Xiang Yu, Chenqi Zhu, Volkan Esenadag , Kean Boon Lee , and Tao Wang 

The University of Sheffield, Sheffield S1 3JD, U.K.

DOI:10.1109/JPHOT.2018.2867821

This work is licensed under a Creative Commons Attribution 3.0 License. For more information, see <http://creativecommons.org/licenses/by/3.0/>

Manuscript received July 26, 2018; revised August 20, 2018; accepted August 23, 2018. Date of publication August 29, 2018; date of current version September 27, 2018. This work was supported by the Engineering and Physical Sciences Research Council of United Kingdoms under Grant EP/P006973/1. Corresponding author: Tao Wang (e-mail: t.wang@sheffield.ac.uk).

Abstract: This paper reports a monolithic integration of GaN high-electron-mobility transistor (HEMT) and green light-emitting diode (LED), where the circular HEMT is surrounded by a ring-shaped LED and two devices are seamlessly interconnected by the LED's n-GaN layer and the HEMT's two-dimensional electron gas (2DEG) channel. By adopting such a novel circular layout design, the green HEMT-LED shows a controllable and uniform green light emission at 507 nm by simply tuning its gate voltage. This enables a uniform, controllable green LED light source, serving as an essential element in the red–green–blue (RGB) LED solution for a wide range of applications, such as tunable-spectrum white LED illumination, multichannel visible light communication with wavelength division multiplexing, RGB-based full-color LED displays, and optogenetics.

Index Terms: Green, HEMT-LED, light emitters.

1. Introduction

It is expected that lighting will ultimately move towards “smart lighting”, meaning that such smart lighting can exhibit multiple functions for not only general illumination but also digitalized applications, where visible light wireless communication such as Light Fidelity (Li-Fi) is a typical example. The key component for smart lighting is a white light-emitting diode (LED) featured with both high efficiency and high data transmission rates. The last two decades have seen major progress in developing white LEDs overwhelmingly based on III-nitride semiconductors. So far, the current state-of-the-art white LEDs mainly based on the well-known “blue LED + yellow phosphor” method have approached their limit in terms of overall performance including both efficiency and color rendering index. However, such phosphor-converted white LEDs are still far from satisfactory. One of the fatal issues is due to the very slow response time of yellow phosphors, typically on the order of microseconds, leading to a limited bandwidth down to several MHz level for Li-Fi applications [1], [2].

In order to achieve the best lighting quality (in terms of both color rendering index and chromaticity) with multiple functions (display, communications, detection, etc.), it is an ideal solution to fabricate white LEDs by mixing individually addressable red, green and blue (RGB) LED components. In that case, three independent RGB components forming a white LED can be modulated using the wavelength division multiplexing (WDM) technology. In [3], by means of the RGB LED approach, a 3.4 Gbit/s data rate has been demonstrated. Furthermore, augmented reality/virtual reality (AR/VR)

requires portable display, where a micro-display with an ultrafast response is required. Therefore, the fabrication of a micro-display using RGB LEDs demonstrates a great potential to offer high color quality and dimmable display pixels [4]. For opto-genetics applications, where the blue/green opsin can be driven by blue and green LEDs [5], a green LED is also an indispensable component which needs to be modulated for opsin excitation.

The above facts indicate that only all the three discrete red, green and blue LED components are well controlled and modulated in an ultra-fast manner can these multiple functions be achieved. Therefore, an electrical channel with an ultrafast speed is necessary for the interconnection between LED driving transistors and individual LED components, for which high electron mobility transistors (HEMTs) are a good option. Therefore, in order to address the above issues, the fabrication of an integrated HEMT-LED is a promising and reliable approach [6].

Except of the bandwidth, a uniform light emission is also necessary for many applications. For instance, the short-distance transmission via plastic optical fiber (POF) also requires a green light source at 500 nm with uniform light emission for the POF systems [7].

So far, the progress on the fabrication of integrated HEMT-LED is limited to the blue spectral range and lateral layout arrangement [11], [12], where the HEMT is located side-by-side to the blue LED. The existing layout will cause serious current crowding and heating issue especially at high injection current. Moreover, there is no any report about the fabrication of an integrated HEMT-LED in the longer wavelength such as green regime. One of the fundamental reasons is due to the well-known “green gap” issue, although great efforts have been invested in order to bridge the gap [8]–[10]. Consequently, it is crucial to develop a uniform green HEMT-LED served as an essential element for the RGB LED approach stated above. In this paper, for the first time, we report a monolithically integrated HEMT-LED with a circular layout arrangement, which can emit uniform green light and be well controlled by its gate voltage.

2. Experimental Details

Among all the approaches developed for monolithically integrating HEMTs with LEDs so far, the metal-interconnection-free scheme reported has demonstrated major advantages in terms of higher reliability and less parasitic effects [12]. In this scheme, the LED can be electrically integrated with an HEMT via the 2DEG channel of the HEMT to form a compact HEMT-LED device. The growth procedure is described as following. First, a GaN HEMT epiwafer is grown on a standard c-plane sapphire substrate by means of a metal-organic vapor phase epitaxy (MOVPE) technique. The GaN HEMT epiwafer is grown by using our high-temperature AlN (HT-AlN) buffer approach [13]. After the sapphire substrate is initially subject to a high temperature annealing process under H₂ ambient, a 600 nm HT-AlN layer is grown, followed by a 1.5 μ m undoped GaN layer, then a 1 nm AlN spacer layer and a final 25 nm Al_{0.25}Ga_{0.75}N barrier layer.

As shown in Fig. 3(a) and (b), in order to prepare a patterned template for further green LED overgrowth, a 500 nm SiO₂ layer is deposited on the HEMT epiwafer by plasma-enhanced chemical vapor deposition (PECVD), and then patterned by a combination of standard lithography technique and subsequent dry etching processes in order to form window regions where a green LED structure will be selectively grown later. Within the window regions, the active region of HEMT epiwafer has been etched down to 300 nm, namely, down to the GaN buffer layer of the HEMT epiwafer.

Subsequently, the patterned template featured with selective etching is reloaded into the MOVPE chamber for further LED growth after a special surface treatment of 5-min photo-assisted KOH etching which aims to remove any damages induced during the dry-etching processes. A 100 nm undoped GaN is initially selectively grown within the window regions for a better n-GaN interface, followed by a 1 μ m n-GaN layer. Three periods of InGaN/GaN multiple quantum wells (MQWs) are then grown, where each quantum well consists of a 2.5 nm InGaN quantum well separated by a 10 nm GaN barrier. Finally, 15 nm p-AlGaN as an electron blocking layer and then a 150 nm p-doped GaN followed by a 5 nm heavily doped GaN capping layer are grown. After

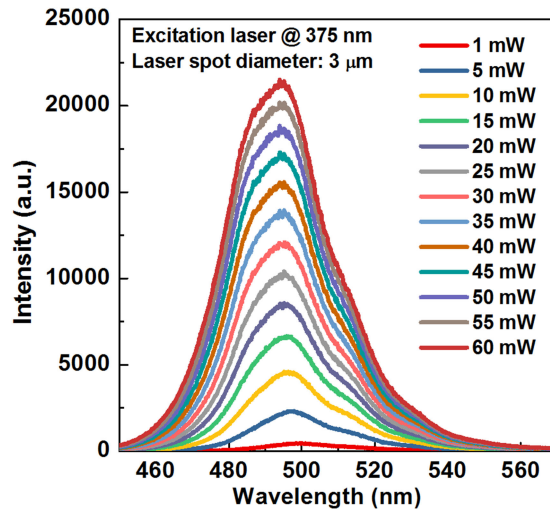


Fig. 1. Excitation-power dependent PL spectra of our overgrown LED epiwafer.

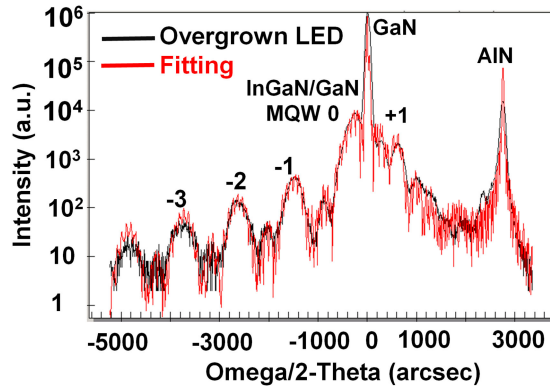


Fig. 2. XRD spectrum of our overgrown LED epiwafer measured in a $2\theta-\omega$ mode.

the selective epitaxial overgrowth, the SiO_2 mask has been completely removed by a 40% HF solution.

X-ray diffraction (XRD) and photoluminescence (PL) measurements have been performed in order to characterize the sample. Fig. 1 shows excitation-power dependent PL spectra, still exhibiting a green emission centered at 500 nm and a clear blue-shift (to 493 nm) under the strong excitation power density increasing from 1.41×10^4 to $8.49 \times 10^5 \text{ W/cm}^2$. Fig. 2 shows the XRD data measured in a $2\theta-\omega$ mode, indicating 2.3 nm InGaN quantum wells with 25% indium content.

Finally, an integrated HEMT-LED device will be fabricated. In the very first step of HEMT-LED fabrication, the HEMT mesa (300 nm) and LED mesa (500 nm) are defined by a standard inductively coupled etching (ICP), respectively. A source/drain Ohmic contact (Ti/Al/Ti/Au: 20/50/150/80 nm) for the HEMT are deposited by thermal evaporation and then annealed in 850°C under N₂ ambient. A Ni/Au layer with their individual thickness of 7 and 7 nm is used as a current spreading layer. A layer of Ti/Al/Ti/Au with their thickness of 20/150/50/50 nm as an electrode for LED and a Schottky contact (Ni/Au: 50/150 nm) for the gate of HEMT are finally deposited. A schematic illustration for the whole fabrication process is depicted in Fig. 3, where the red dash line represents the 2DEG channel serving as an interconnection between the HEMT and the green LED.

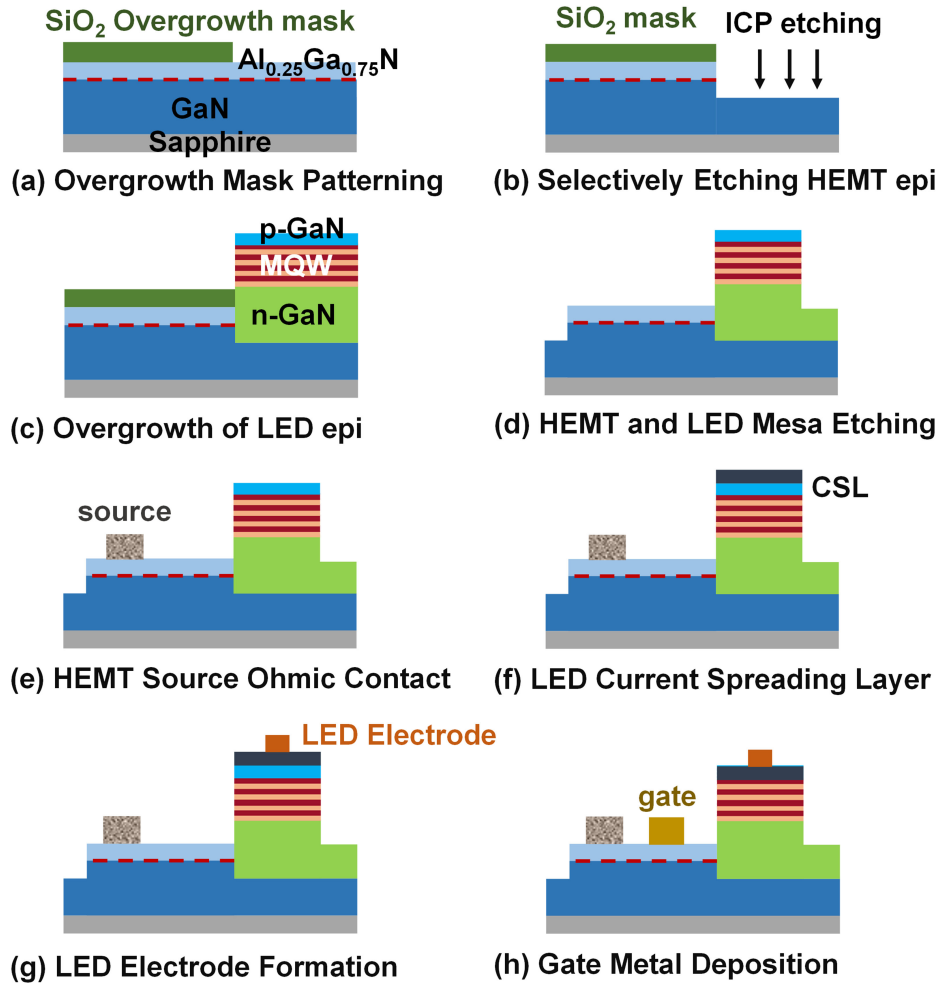


Fig. 3. Schematic illustration of fabrication processes of our green HEMT-LED devices.

3. Results

Fig. 4(a)–(c) show the optical microscope image and the layout of our green HEMT-LED device, respectively. A circular layout design is adopted, meaning that the ring-shaped LED surrounds the HEMT in order to facilitate current spreading. For the ring-shaped LED, the inner and outer diameter are $140\ \mu\text{m}$ and $600\ \mu\text{m}$, respectively. As for the HEMT driving transistor's layout parameters shown in Fig. 4(c), source diameter (R_s), gate length (L_s), gate-to-source distance (L_{gs}), gate-to-drain distance (L_{gd}) and gate width (W_g) are 40 , 4 , 6 , 20 and $300\ \mu\text{m}$, respectively. Fig. 4(b) shows our green HEMT-LED device in three dimensions (3D), where a finger-shaped circular electrode is designed for the green LED in order to facilitate current spreading. The current can be injected from the ring-shaped anode of LED into the n-GaN layer uniformly, to the 2DEG channel of HEMT and finally sink into the source of HEMT. The circular HEMT is surrounded by the LED mesa and used for modulating or controlling the LED current. The benefit of such circular layout is that it can achieve better current spreading and less heating issues compared with the previously reported side-by-side lateral HEMT-LED layout, especially at high injection current [14]–[17].

Fig. 5 shows current-voltage (I-V) and transfer characteristics of our integrated green HEMT-LED devices, indicating a turn-on voltage of $3\ \text{V}$, which is reasonable considering the serially connected LED diode to the drain terminal of the HEMT. The maximum current density and trans conductance for HEMT is $35\ \text{mA}/\text{mm}$ and $16.7\ \text{mS}/\text{mm}$, respectively. The whole HEMT-LED device shows a static

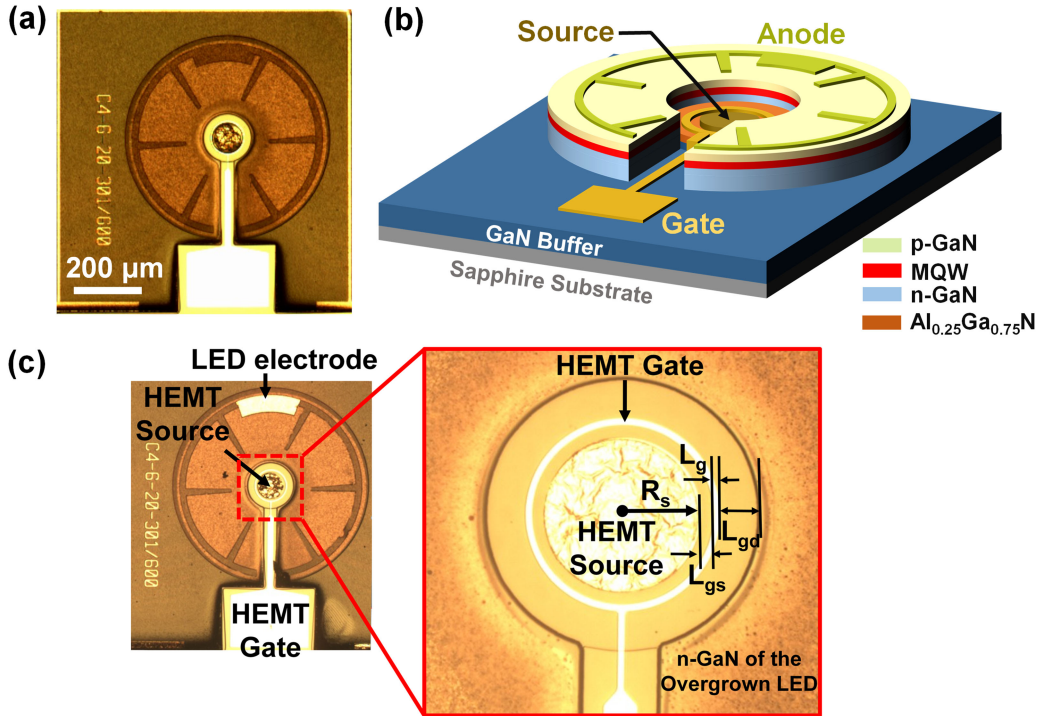


Fig. 4. (a) Optical microscope image of our HEMT-LED devices. (b) Schematic illustration of our device in 3D. (c) Layout parameters for the integrated HEMT.

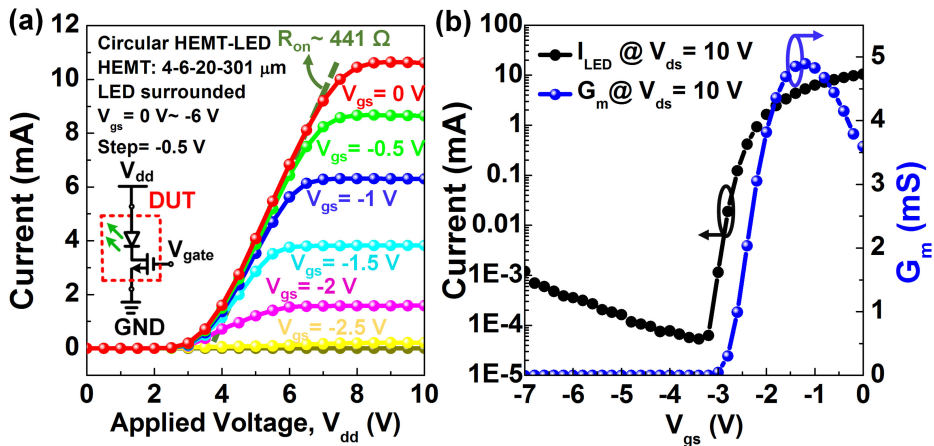


Fig. 5. HEMT-LED devices (a) I-V (inset: an equivalent circuit of HEMT-LED). (b) Transfer characteristics.

on resistance of 441Ω , including the on resistance of $300 \mu\text{m}$ -width HEMT and the ring-shaped LED. Since the current of HEMT-LED can be simply tuned by its gate voltage, the HEMT-LED itself can be used as a modulated light source. Fig. 6(a) and (b) show an electroluminescence (EL) emission image taken at 1 mA and EL spectra as a function of injection current, respectively. A very uniform green light emission has been achieved. Fig. 6(b) shows a peak wavelength shifting from 507.5 nm to 503.5 nm when the injection current increases from 1 to 6 mA .

At the moment, the HEMT features a low maximum current density (35 mA/mm^2), almost one order smaller than the reported current density of GaN HEMT [18]. Further investigation is ongoing in order to identify whether the low current is due to either overgrowth or dry-etching induced

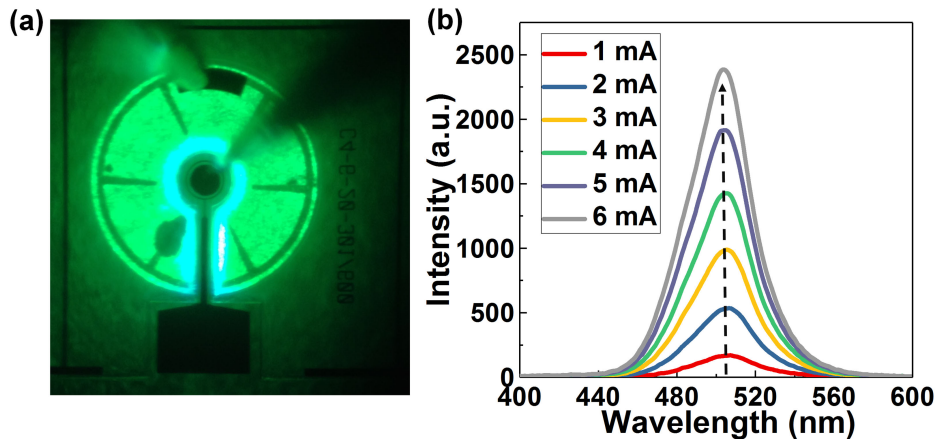


Fig. 6. (a) EL emission image taken at 1 mA. (b) EL spectra as a function of injection current.

damages. It should be noted that a low growth temperature for the overgrowth of InGaN/GaN MQWs is required in order to achieve green emission.

4. Conclusion

To conclude, we have demonstrated a prototype green HEMT-LED device with uniform light emission at 507 nm. The ring-shaped LED can be driven and well controlled by the integrated circular HEMT through simply tuning the gate voltage of HEMT. This controllable uniform green HEMT-LED device paves the way for applying the RGB-LED solution in fabricating smart lighting devices for many practical applications where controllable green LEDs are an essential component, such as tunable spectrum white LED for high-quality lighting, three-channel visible light communication for Li-Fi, full color LED displays for AR/VR and optogenetics for biomedical diagnosis.

References

- [1] J. Grubor, S. C. J. Lee, K. D. Langer, T. Koonen, and J. W. Walewski, "Wireless high-speed data transmission with phosphorescent white-light LEDs," in *Proc. 33rd Eur. Conf. Exhib. Opt. Commun.*, 2007, pp. 1–2.
- [2] M. Biagi, T. Borogovac, and T. D. C. Little, "Adaptive receiver for indoor visible light communications," *J. Lightw. Technol.*, vol. 31, no. 23, pp. 3676–3686, Dec. 2013.
- [3] G. Cossu, A. M. Khalid, P. Choudhury, R. Corsini, and E. Ciaramella, "3.4 Gbit/s visible optical wireless transmission based on RGB LED," *Opt. Express*, vol. 20, no. 26, pp. B501–B506, 2012.
- [4] J. Day, J. Li, D. Y. C. Lie, C. Bradford, J. Y. Lin, and H. X. Jiang, "III-Nitride full-scale high-resolution microdisplays," *Appl. Phys. Lett.*, vol. 99, no. 3, 2011, Art. no. 031116.
- [5] A. Guru, R. J. Post, Y.-Y. Ho, and M. R. Warden, "Making sense of optogenetics," *Int. J. Neuropsychopharmacol.*, vol. 18, no. 11, 2015, Art. no. pyv079.
- [6] Y. Cai, X. Zou, C. Liu, and K. M. Lau, "Voltage-controlled GaN HEMT-LED devices as fast-switching and dimmable light emitters," *IEEE Electron Device Lett.*, vol. 39, no. 2, pp. 224–227, Feb. 2018.
- [7] C. L. Liao, C. L. Ho, Y. F. Chang, C. H. Wu, and M. C. Wu, "High-speed light-emitting diodes emitting at 500 nm with 463-MHz modulation bandwidth," *IEEE Electron Device Lett.*, vol. 35, no. 5, pp. 563–565, May 2014.
- [8] S. Karpov, "Effect of carrier localization on recombination processes and efficiency of InGaN-Based LEDs operating in the "green gap"," *Appl. Sci.*, vol. 8, no. 5, 2018, Art. no. 818.
- [9] Y. Jiang *et al.*, "Realization of high-luminous-efficiency InGaN light-emitting diodes in the "green gap" range," *Sci. Rep.*, vol. 5, 2015, Art. no. 10883.
- [10] A. I. Alhassan *et al.*, "High luminous efficacy green light-emitting diodes with AlGaN cap layer," *Opt. Express*, vol. 24, no. 16, pp. 17868–17873, 2016.
- [11] C. Liu, Y. Cai, X. Zou, and K. M. Lau, "Low-leakage high-breakdown laterally integrated HEMT-LED via n-GaN electrode," *IEEE Photon. Technol. Lett.*, vol. 28, no. 10, pp. 1130–1133, May 2016.
- [12] C. Liu, Y. Cai, Z. Liu, J. Ma, and K. M. Lau, "Metal-interconnection-free integration of InGaN/GaN light emitting diodes with AlGaN/GaN high electron mobility transistors," *Appl. Phys. Lett.*, vol. 106, no. 18, 2015, Art. no. 181110.
- [13] Y. Gong, K. Xing, and T. Wang, "Influence of high temperature AlN buffer on optical gain in AlGaN/AlGaN multiple quantum well structures," *Appl. Phys. Lett.*, vol. 99, no. 17, 2011, Art. no. 171912.

- [14] A. Porch, D. V. Morgan, R. M. Perks, M. O. Jones, and P. P. Edwards, "Transparent current spreading layers for optoelectronic devices," *J. Appl. Phys.*, vol. 96, no. 8, pp. 4211–4218, 2004.
- [15] Y. Cai, X. Zou, W. C. Chong, and K. M. Lau, "Optimization of electrode structure for flip-chip HVLED via two-level metallization," *Physica Status Solidi (a)*, vol. 213, no. 5, pp. 1199–1203, 2016.
- [16] H. Hsin-Hui *et al.*, "Characterization of RF lateral-diffused metal–oxide–semiconductor field-effect transistors with different layout structures," *Jpn. J. Appl. Phys.*, vol. 46, no. 4S, 2007, Art. no. 2032.
- [17] A. M. Darwish, H. A. Hung, and A. A. Ibrahim, "A ring-HEMT for improved GaN MMIC thermal dissipation," in *Proc. Int. Symp. IEEE MTT-S Microw.*, 2013, pp. 1–3, doi: [10.1109/MWSYM.2013.6697631](https://doi.org/10.1109/MWSYM.2013.6697631).
- [18] L. Shen *et al.*, "High-power polarization-engineered GaN/AlGaN/GaN HEMTs without surface passivation," *IEEE Electron Device Lett.*, vol. 25, no. 1, pp. 7–9, Jan. 2004.